Phospholipids with a Stimuli-Responsive Thermotropic Liquid-Crystalline Moiety

Kiyoshi Kanie,[a]* Junji Sekiguchi,[a] Xiangbing Zeng,[b] Goran Ungar,[b] and Atsushi Muramatsu[a]

[a]*Institute of Multidisciplinary Research for Advanced Materials, Tohoku University*

Katahira 2-1-1, Aoba-ku, Sendai 980-8577, Japan

[b]*Department of Engineering Materials, University of Sheffield,*

Mappin St., Sheffield S1 3JD, UK

Electric Supplementary Information

1. General

All reagents of the highest commercial quality and solvents (Aldrich Chemicals, Wako Pure Chemicals, Nakalai Tesque, Kanto Chemicals, or Tokyo Kasei) were used as received. Water was doubly distilled and deionized prior to use. All of the organic reactions were carried out under an argon atmosphere in a dry solvent. Glass vessels for the organic reactions were well-dried by heating under reduced pressure. Completion of the reactions was monitored by thin-layer chromatography using 0.25 mm E. Merck silica-gel plates (Silica Gel F254) were used, and were visualized by UV light and/or by dipping the plates in an ethanolic sodium phosphomolybdate followed by heating. Purification of phospholipids containing a thremotropic liquid-crystalline moiety prepared in the present study was carried out by Yamazen Fast Flow Liquid Chromatography system using High-Flash columns (SiO_2 and ODS).

Measurements of phase transition temperatures and determinations of liquid-crystalline phases were carried out with an Olympus BX51 optical polarizing microscope equipped with a Mettler FP82 HT hot stage or with a custom-made high pressure hot stage. Thermal characterization was performed with a TA Instruments MDSC Q-100 equipped with a refrigerated cooling system. The scanning rate was 10 °C/min. To prevent evaporation of solvents, high pressure capsule kit was used for the DSC measurements. Infrared (IR) spectra were conducted on a Bruker FTS-7000 equipped with a microscope UMA-600. IR measurements for characterization of molecules were carried out by using an ATR unit. NMR spectra were measured in a CD_3OD solution unless otherwise noted. ^{1}H and ^{13}C NMR spectra were recorded on a JEOL JNM-LA400 at 400 (^{1}H) and 100.7 (^{13}C) MHz. Chemical shifts of ^{1}H NMR signals were quoted to internal standard Me_4Si ($\delta = 0.00$) and expressed as chemical shifts in ppm (δ), multiplicity, coupling constant (Hz), and relative intensity. Chemical shifts of ^{13}C NMR signals were quoted to internal standard CD_3OD ($\delta = 49.00$) and listed as chemical shifts in ppm (δ). High resolution mass spectra (HRMS) were recorded on a Bruker FT-MS APEXIII spectrometer by using electron spray ionization (ESI) mode. Elemental analyses were carried out by Elemental Analysis Laboratory, Institute of Multidisciplinary Research for Advanced Materials, Tohoku University, using a Yanako MT-6 CHN Corder. Temperature dependent small angle X-ray scattering (SAXS) measurements were carried out using a Rigaku Nano-viewer system equipped with a Mettler FP82 HT hot stage.

2. Synthesis of Organic Molecules

2-1. Preparation of 4-{*trans*-4-[*trans*-4-(3,4-Difluorophenyl)cyclohexyl]cyclohexyl} butyl phosphocholine (L1b)

Preparation of **L1b** was carried out by the route as shown in Equation S1.

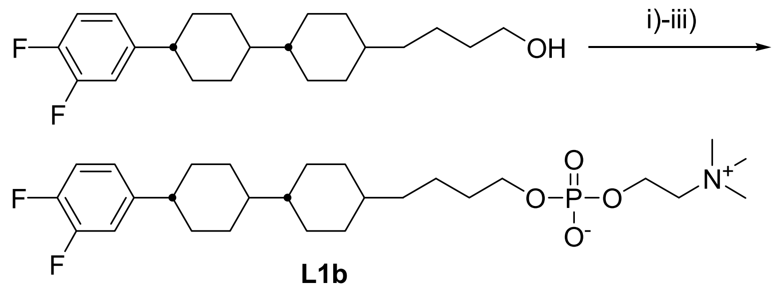

i) $POCl_3$ (1.2 mol), Et_3N (2.0 mol), $CHCl_3$, 0 °C, 2 h;
ii) Choline tosylate (1.5 mol), pyridine, 0 °C to rt, 1 day; iii) H_2O, rt, 30 min.

Equation S1. Synthesis of Mesogenic Molecule **L1b**.

The procedure is as follows: To a solution of phosphorus oxychloride (1.1 mL, 20 mmol) in dry $CHCl_3$ (10 mL), a mixed solution of *trans*-4-[*trans*-4-(3,4-difluorophenyl)cyclohexyl]cyclohexane butanol[S1] (3.5 g, 10.0 mmol) and triethylamine (2.8 mL, 20 mmol) in dry $CHCl_3$ (10 mL) was added dropwise at 0 °C over 10 min with stirring under an argon atmosphere. After 2 h, pyridine (5 mL) and choline tosylate (4.13 g, 15 mmol) were added to the solution at 0 °C, the resulting solution was allowed to warm to room temperature over 30 min, and stirred at the temperature for overnight. Then, water (0.5 mL) was added to the mixture, and the stirring was continued for an additional 30 min. The resulting mixture was concentrated under reduced pressure. The residue was purified by flash column chromatography on Silica gel (eluent: $CHCl_3$: MeOH = 3 : 1 to 1 : 1; then MeOH) followed by on ODS (eluent: 80% aqueous MeOH) to give **L1b** in a yield of 45% (2.3 g, 4.5 mmol) as white powders.

Compound **L1b**: $C_{27}H_{44}F_2NO_4P$. IR (ATR) 3369, 3026, 2918, 2849, 1606, 1516, 1486, 1446, 1247, 1088, 1057, 966, 954, 823, 751 cm^{-1}; ^{1}H NMR (400 MHz) δ = 0.84-1.44 (m, 13 H), 1.58-1.66 (m, 2 H), 1.74-1.89 (m, 8 H), 2.39 (tt, *J* = 3, 12 Hz, 1 H), 3.23 (s, 9 H), 3.30-3.32 (m, 2 H), 3.63-3.66 (m, 2 H), 3.68-3.85 (m, 2 H), 4.22-4.29 (m, 2 H), 6.95-6.99 (m, 1 H), 7.04-7.15 (m, 2 H); ^{13}C NMR (100 MHz) δ = 24.3, 31.2, 31.4, 34.7, 35.7, 38.3, 39.2, 44.1, 44.7, 45.2, 54.6-54.7 (m), 60.3 (d, *J* = 5 Hz), 67.0 (d, *J* = 6 Hz), 67.3-67.5 (m), 116.4 (d, *J* = 16 Hz), 117.8 (d, *J* = 17 Hz), 124.0, (dd, *J* = 3, 6 Hz), 146.6 (dd, *J* = 4, 4 Hz), 149.7 (dd, *J* = 13, 243 Hz), 151.3 (dd, *J* = 13, 244 Hz); HRMS calcd for $[C_{27}H_{44}F_2NO_4P+H]^+$: 516.3049. Found: 516.3048; $[C_{27}H_{44}F_2NO_4P+Na]^+$: 538.2868. Found: 538.2866. Elemental anal. calcd for $C_{27}H_{44}F_2NO_4P{\cdot}0.5H_2O$: C, 61.81; H, 8.65; N, 2.67%. Found: C, 61.72; H, 8.59; N, 2.64%.

2-2. Synthesis of 4-{*trans*-4-[*trans*-4-(3,4-difluorophenyl)cyclohexyl]cyclohexyl} ethyl phosphocholine (L1a)

Synthesis of **L1a** was carried out by the same way for the preparation of **L1b** starting from *trans*-4-[*trans*-4-(3,4-difluorophenyl)cyclohexyl]cyclohexane ethanol.[S1]

Compound **L1a**: Obtained in 66%. $C_{25}H_{40}F_2NO_4P$. IR (ATR) 3355, 3027, 2920, 2851, 1607, 1518, 1446, 1274, 1245, 1085, 1055, 1033, 966, 939, 823, 751 cm^{-1}; ^{1}H NMR (400 MHz) δ = 0.84-1.46 (m, 8 H), 1.53-1.60 (m, 2 H), 1.75-1.92 (m, 8 H), 2.39 (tt, *J* = 3, 12 Hz, 1 H), 3.30 (s, 9 H), 3.69-3.75 (m, 2 H), 3.95-4.02 (m, 2 H), 4.30-4.37 (m, 2 H), 6.95-7.00 (m, 1 H), 7.06-7.15 (m, 2 H); ^{13}C NMR (100 MHz) δ = 31.1, 31.3, 34.5, 35.66, 35.73, 39.3 (d, *J* = 7 Hz), 44.0, 44.5, 45.1, 54.6-54.7 (m), 60.3 (d, *J* = 5 Hz), 64.9 (d, *J* = 6 Hz), 67.3-67.5 (m), 116.3 (d, *J* = 17 Hz), 117.8 (d, *J* = 17 Hz), 124.0, (dd, *J* = 3, 6 Hz), 146.5 (dd, *J* = 4, 4 Hz), 149.7 (dd, *J* = 12, 242 Hz), 151.3 (dd, *J* = 12, 244 Hz); HRMS calcd for $[C_{25}H_{40}F_2NO_4P+H]^+$: 488.2736. Found: 488.2735; $[C_{25}H_{40}F_2NO_4P+Na]^+$: 510.2555. Found: 510.2554. Elemental anal. calcd for $C_{25}H_{40}F_2NO_4P{\cdot}H_2O$: C, 59.39; H, 8.37; N, 2.77%. Found: C, 59.50; H, 8.21; N, 2.77%.

2-3. Preparation of 4-[4-(4-cyano-phenylazo)phenyloxy]propyl phosphocholine (L2a).

Compound **L2a** was obtained by the similar route as shown in equation S1 starting from the corresponding alcohol in a yield of 30% after purification by reversed-phase HPLC using an ODS column (Wakosil-II).

Compound **L2a**: $C_{21}H_{27}N_4O_5P$. IR (ATR) 3328, 3253, 3038, 2966, 2894, 2226, 1600, 1583, 1498, 1418, 1402, 1217, 1142, 1086, 1045, 966, 920, 840, 793, 683 cm^{-1}; ^{1}H NMR (400 MHz) δ = 2.11-2.18 (m, 2 H), 3.30 (s, 9 H), 3.56-3.62 (m, 2 H), 4.05-4.14 (m, 2 H), 4.20-4.25 (m, 4 H), 7.11 (d, *J* = 9 Hz, 2 H), 7.87 (d, *J* = 9 Hz, 2 H), 7.94 (d, *J* = 9 Hz, 2 H), 7.96 (d, *J* = 9 Hz, 2 H); ^{13}C NMR (100 MHz) δ = 31.5 (d, *J* = 7 Hz), 54.6 (t, *J* = 4 Hz), 60.3 (d, *J* = 5 Hz), 63.3 (d, *J* = 6 Hz), 66.0, 67.4 (m), 69.4, 114.4, 116.1, 119.5, 124.2, 126.5, 134.5, 148.2, 156.2, 164.1; HRMS calcd for $[C_{21}H_{27}N_4O_5P+H]^+$: 447.1792. Found: 447.1792; $[C_{21}H_{27}N_4O_5P+Na]^+$: 469.1611. Found: 469.1610. Elemental anal. calcd for $C_{21}H_{27}N_4O_5P{\cdot}1.5H_2O$: C, 53.29; H, 6.38; N, 11.83%. Found: C, 53.38; H, 6.30; N, 11.65%.

2-4. Synthesis of 4-[4-(4-cyano-phenylazo)phenyloxy]hexyl phosphocholine (L2b).

Preparation of **L2b** was performed by the same route as shown in Equation S1.

Compound **L2b**: Obtained in 28%. $C_{24}H_{33}N_4O_5P$. IR (ATR) 3327, 3267, 3039, 2947, 2877, 2226, 1602, 1584, 1501, 1470, 1417, 1235, 1143, 1073, 1051, 1019, 967, 836, 791, 756 cm^{-1}; ^{1}H NMR (400 MHz) δ = 1.49-1.63 (m, 4 H), 1.72-1.79 (m, 2 H), 1.84-1.91 (m, 2 H), 3.30 (s, 9 H), 3.68-3.73 (m, 2 H), 3.95-4.00 (m, 2 H), 4.11 (t, *J* = 6 Hz, 2 H), 4.30-4.36 (m, 2 H), 7.10 (d, *J* = 9 Hz, 2 H), 7.90 (d, *J* = 9 Hz, 2 H), 7.95 (d, *J* = 9 Hz, 2 H), 7.98 (d, *J* = 9 Hz, 2 H); ^{13}C NMR (100 MHz) δ = 26.6, 26.8, 31.7 (d, *J* = 7 Hz), 54.7 (t, *J* = 3 Hz), 60.2 (d, *J* = 5 Hz), 66.8 (d, *J* = 6 Hz), 67.4 (m), 69.4, 114.2, 116.0, 119.5, 124.1, 126.5, 134.4, 147.9, 156.1, 164.2; HRMS calcd for $[C_{24}H_{33}N_4O_5P+H]^+$: 489.2261. Found: 489.2262; $[C_{24}H_{33}N_4O_5P+Na]^+$: 511.2081. Found: 511.2079. Elemental anal. calcd for $C_{24}H_{33}N_4O_5P{\cdot}H_2O$: C, 56.91; H, 6.96; N, 11.06%. Found: C, 56.92; H, 6.75; N, 10.94%.

3. Structure Characterization of Lyotropic LC Phase Structures of L1a and L1b

Diffraction intensities were Lorentz and multiplicity corrected. Fourier reconstruction of the electron density is carried out using the general formula for columnar phases (2-dimensional order):

$$\rho(xy) = \Sigma_{hk} F(hk) \exp[2\pi i(hx+ky)] = \Sigma_{hk} \sqrt{I(hk)} \exp[2\pi i(hx+ky) + i\phi(hk)]$$

Here $\phi(hk)$ is the phase of the (hk) reflection and I is the corrected intensity. In the tables below the phase is labeled + for $\phi(hk) = 0$ and – for $\phi(hk) = \pi$.

3-1. The H_2O/L1b = 1.5 (wt/wt) System

The diffraction pattern of the H_2O/**L1b** = 1.5 (wt/wt) system at 40 °C can be indexed on a rectangular lattice with parameters of a = 126.9 Å; b = 98.6 Å, plane group *p2gg*. Table S1 lists the measured and calculated scattring vector values (q) along with the experimental intensities, calculated intensities and phases for the best fit model.

Table S1. Measured and calculated scattering vectors and integrated and calculated intensities of a *p2gg* phase of the H_2O/**L1b** = 1.5 (wt/wt) system at 40 °C.

h	k	q (Å^{-1}) calc.	q (Å^{-1}) exp.	Intensity exp.	Intensity calc.	Phase
1	1	0.081	0.081	100	100.1	–
2	0	0.099	0.099	15	15.0	–
2	1	0.118	0.118	48	47.8	–
0	2	0.128	0.128	9.5	9.5	+

The reconstructed electron density map and the best-fit model of the self-assembled structure of **L1b** are shown in Fig. S1.

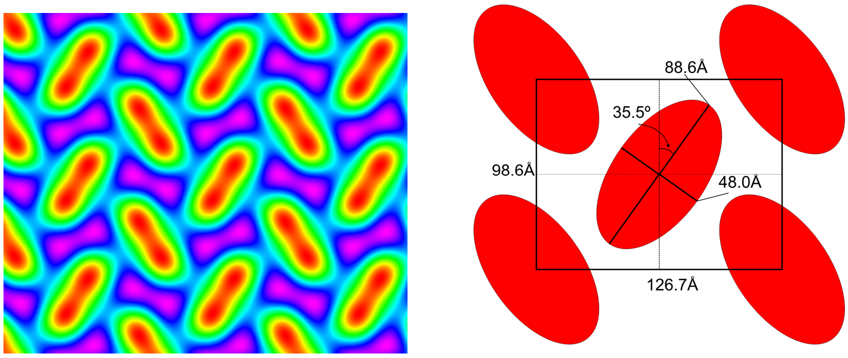

Fig. S1 Reconstructed electron density map of the H_2O/**L1b** = 1.5 (wt/wt) system at 40 °C and the best-fit model of the self-assembled elliptical cylinder structure of **L1b**.

3-2. The H_2O/L1a = 1.0 (wt/wt) System

Table S2 summarizes the measured and calculated scattring vectors (q) of the *hk* reflections, along with the experimental intensities, calculated intensities and phases for the best fit model. The unit cell is rectangular, with parameters a = 91.7 Å, b = 72.6 Å; plane group: *p2gg*.

Table S2. Measured and calculated scattering vectors and integrated and calculated intensities of the *p2gg* phase of the H_2O/**L1a** = 1.0 (wt/wt) system at 40 °C.

h	k	q (Å^{-1}) calc.	q (Å^{-1}) exp.	Intensity exp.	Intensity calc.	Phase
1	1	0.110	0.110	100	101.2	–
2	0	0.137	0.137	25	23.5	–
2	1	0.162	0.162	45	46.1	–
0	2	0.173	0.173	12	13.2	+
1	2	0.186	Not observed		0.3	+
3	1	0.223	0.223	11	6.4	+
2	2	0.221			3.9	+
3	2	0.269	0.269	15	14.6	+
1	3	0.268			2.1	–
4	0	0.274	Not observed		3.2	+
4	1	0.287	0.289	20	11.1	+
2	3	0.293			0.7	+

Reconstructed electron density map using the first 4 diffraction orders are shown in Figure S2 on the left. The structure factor phases used are given in Table S2. For fitting of the diffraction intensities a bi-electron density model (one constant for surfactant, the other for water) is used. The cross-section of the surfactant cylinder is assumed to be elliptical, and three fitting parameters are used: the long and the short half-axes of the ellipse and the setting angle. The best-fit model, including the values of the best fit parameters, is shown in Fig. S2 on the right.

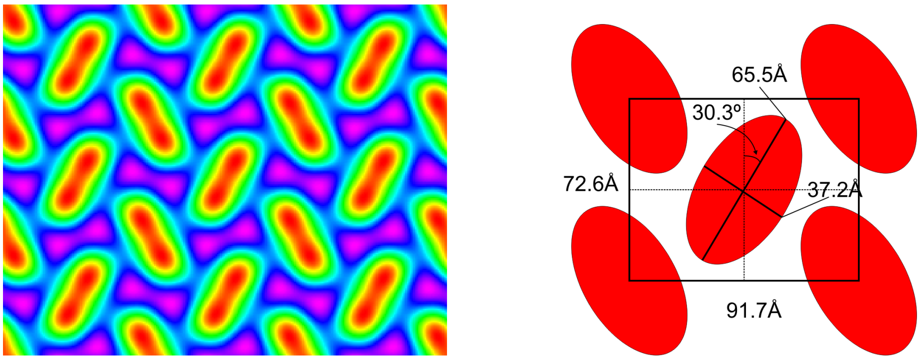

Fig. S2 Reconstructed electron density map of the H_2O/**L1a** = 1.0 (wt/wt) system at 40 °C and the best-fit model of the self-assembled elliptical cylinder structure.

Fig. S3 shows the comparison of the experimental and calculated powder diffraction patterns of the H_2O/**L1a** = 1.0 (wt/wt) system at 40 °C . Peak positions as well as intensities of the calculated pattern are in good agreement with the experimental pattern.

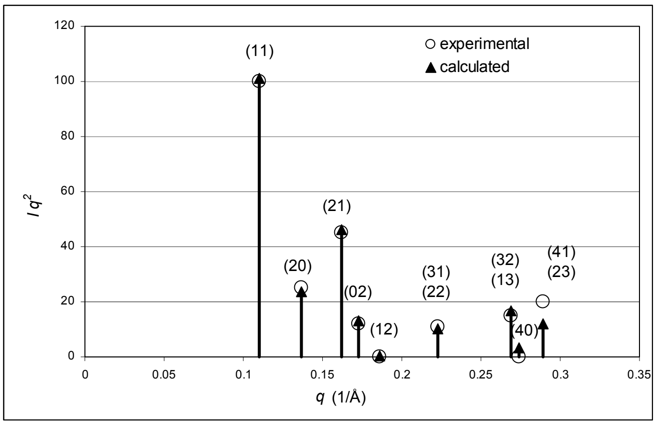

Fig. S3 Comparison of the experimental and calculated diffraction pattern of the H_2O/**L1a** = 1.0 (wt/wt) system at 40 °C.

4. X-ray Single Crystal Structure of L1a

For the evaluation of the lyotropic LC self-assembled structure of **L**, X-ray single crystal structure analysis of **L1a** was carried out. The single crystal was obtained by slow evaporation of methanolic solution of **L1a**. The crystal data were collected by a Rigaku Saturn system using Mo Kα irradiation, and the crystal structure was analyzed using Rigaku CrystalStructure 3.8.0. Single Crystal Structure Analysis Software. The refined data for **L1a** are as follows: Triclinic, space group *P*-1 (No. 2), $C_{25}H_{40}F_2NO_4P$

1/2 CH_3OH; a = 11.057, b = 12.834, c = 19.130 Å, α = 95.729 °, β = 90.211 °, γ = 99.258 °; V = 2665.5 Å^3; Z = 4; R = 0.0405, wR = 0.0996.

Fig. S4 shows the structure of **L1a** viewed along a-, b-, and c-axes. Compound **L1a** forms tilted monolayers in the crystalline phase.

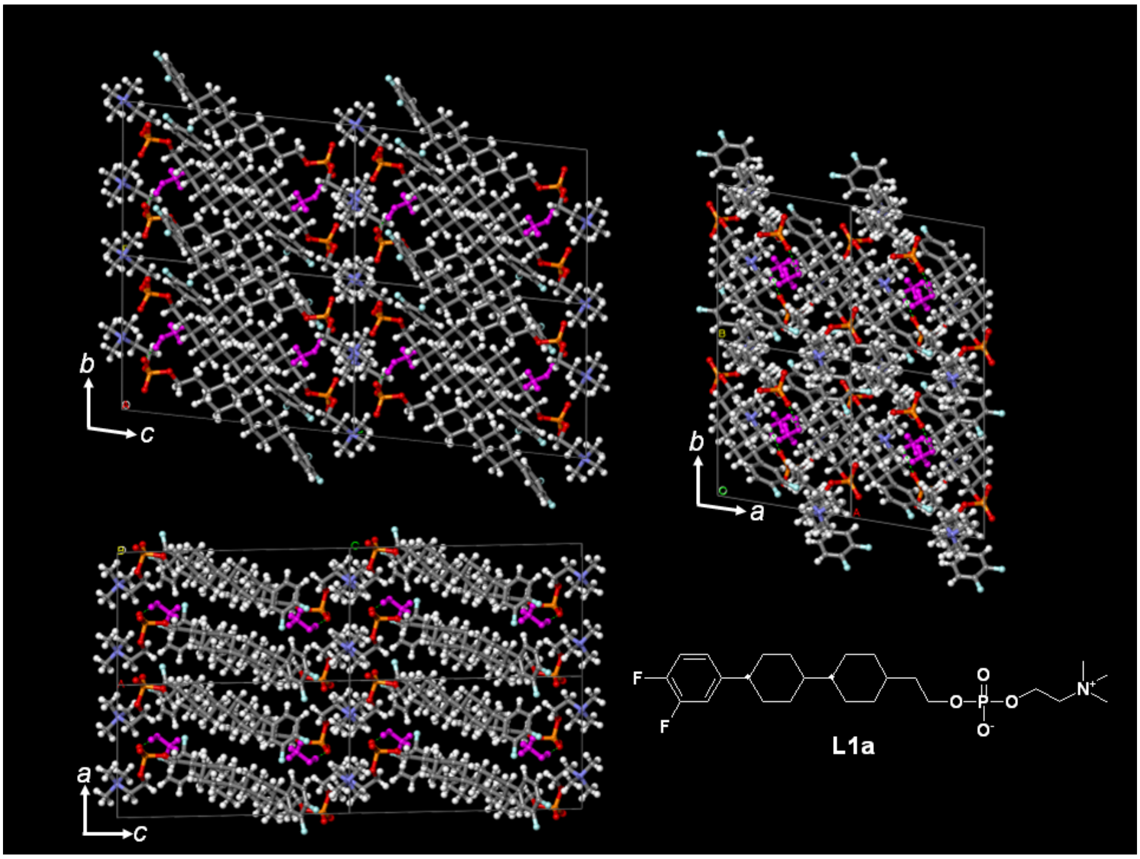

Fig. S4 The X-ray single crystal structure of **L1a.**

References for ESI

(S1) Kanie, K.; Takehara, S.; Hiyama, T. *Bull. Chem. Soc. Jpn.*, **2000**, *73*, 1875.